SUPPLEMENTAL DATA

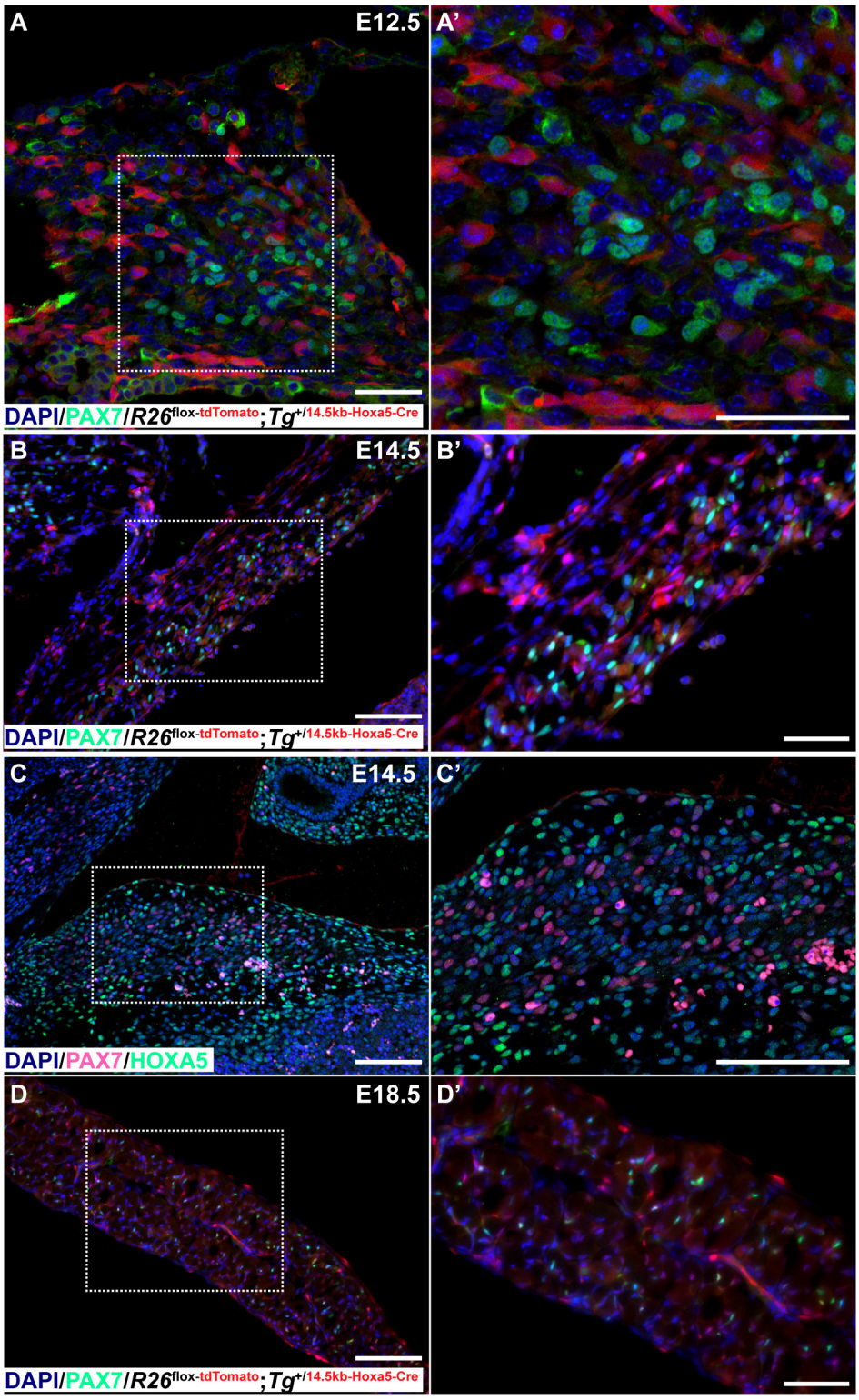

Figure S1

Figure S1. *Hoxa5* is not expressed in muscle cells of the diaphragm. PAX7 immunostaining was performed on sections of the developing diaphragm from E12.5 (A-A'), E14.5 (B-B') and E18.5 (D-D') *R26*^{mT};*Hoxa5-Cre* embryos. No PAX7 co-staining was observed in *Hoxa5* descendant cells (*R26*^{mT}-positive). PAX7 and HOXA5 co-immunolabelling was also performed on diaphragm sections from E14.5 wt embryos and no co-staining was observed (C-C'). Scale bars: 100 µm (B,D), 50 µm (B',C-C',D'), 25 µm (A-A').

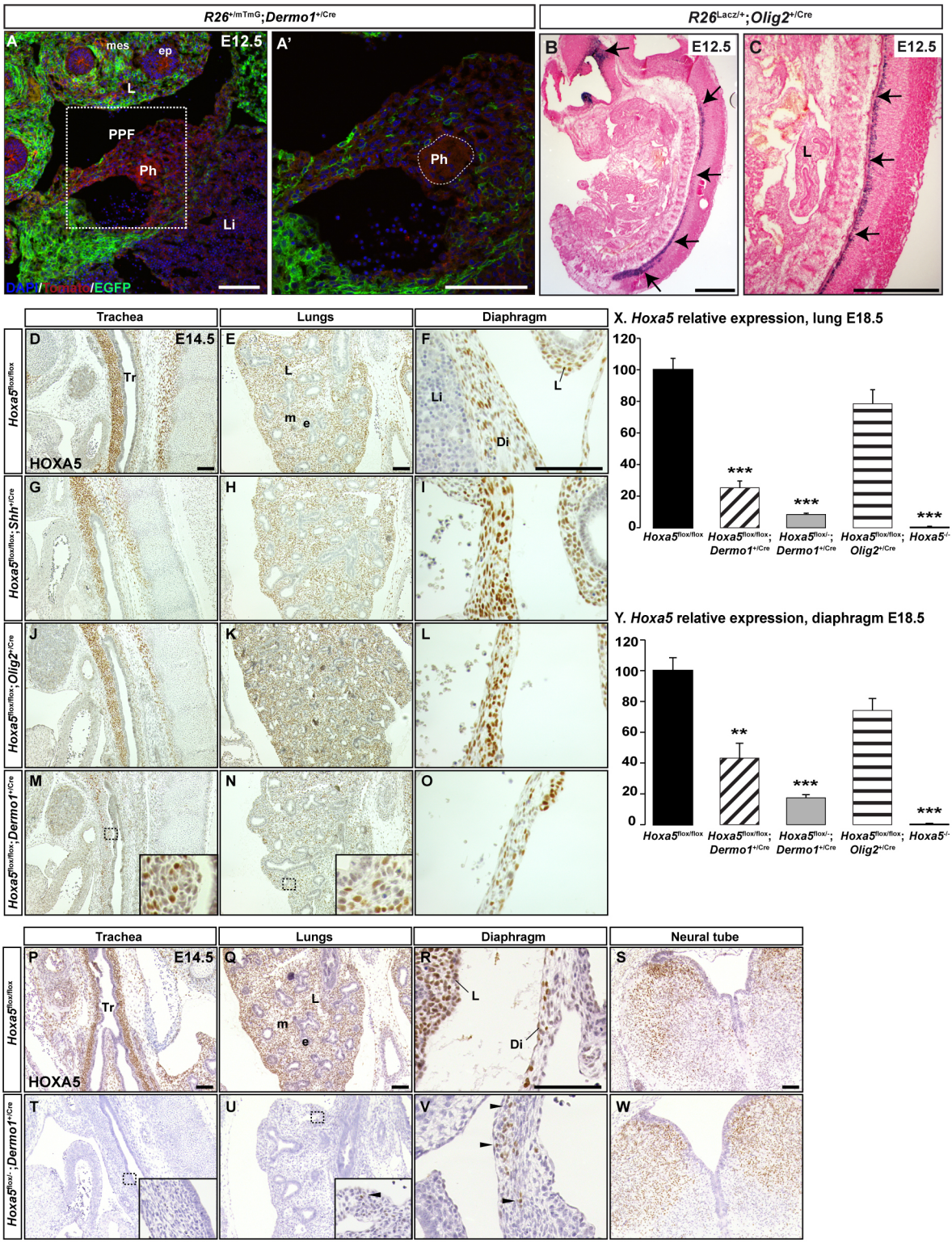

Figure S2

Figure S2. Cre recombinase specificity and efficiency of the *Hoxa5* deletion by the *Shh*^{Cre} , *Dermo1*^{Cre} and *Olig2*^{Cre} alleles in the developing respiratory system. Validation of Cre specificity was assessed by breeding *Dermo1*$^{+/Cre}$ and *Olig2*$^{+/Cre}$ mice with *R26*$^{mT/mG}$ and *R26*$^{+/LacZ}$ reporter mice, respectively. Dermo1Cre activity was assayed by GFP visualization on sections of E12.5 *R26*$^{mT/mG}$;*Dermo1*$^{+/Cre}$ embryos (A-A'). Olig2Cre activity was monitored by β-galactosidase staining in sections of E12.5 *R26*$^{+/LacZ}$;*Olig2*$^{+/Cre}$ embryos (B,C). Efficiency of the *Hoxa5* deletion with the *Shh*^{Cre}, *Dermo1*^{Cre} and *Olig2*^{Cre} alleles in the developing trachea, lung and diaphragm was tested by IHC at E14.5 (D-W). As expected, HOXA5 mesenchymal expression was not affected by ShhCre and Olig2Cre recombinases (G-L), whereas the efficiency of the Dermo1Cre was incomplete and residual HOXA5 expression remained (M-O, P-W). Efficiency of the *Hoxa5* deletion in lung and diaphragm was also monitored by qRT-PCR at E18.5 (X-Y). A significant 75% and 57% reduction was observed in *Hoxa5*$^{flox/flox}$;*Dermo1*$^{+/Cre}$ lung and diaphragm, respectively. The reduction was more important in *Hoxa5*$^{flox/-}$;*Dermo1*$^{+/Cre}$ specimens. No significant variation was seen in E18.5 *Hoxa5*$^{flox/flox}$;*Olig2*$^{+/Cre}$ lungs and diaphragm but a complete loss of *Hoxa5* expression was measured in *Hoxa5*$^{-/-}$ specimens. Di, diaphragm; ep, epithelium; L, lungs; Li, liver; mes, mesenchyme; Ph, phrenic nerve; Tr, trachea. Scale bars: 1 mm (B,C), 100 μm (D-W), 50 μm (A-A').

A. Ratio of genotypes of offspring from *Hoxa5*$^{flox/+}$;*Shh*$^{+/Cre}$ x *Hoxa5*$^{flox/flox}$

			Shh $^{+/+}$		*Shh* $^{+/Cre}$	
Age	**# of litters**	**# of animals**	***Hoxa5*** $^{flox/+}$	***Hoxa5*** $^{flox/flox}$	***Hoxa5*** $^{flox/+}$	***Hoxa5*** $^{flox/flox}$
E18.5	9	59 (100%)	12 (21%)	15 (25%)	15 (25%)	17 (29%)
P30	7	47 (100%)	10 (21%)	17 (36%)	7 (15%)	13 (28%)
% Expected			**25%**	**25%**	**25%**	**25%**

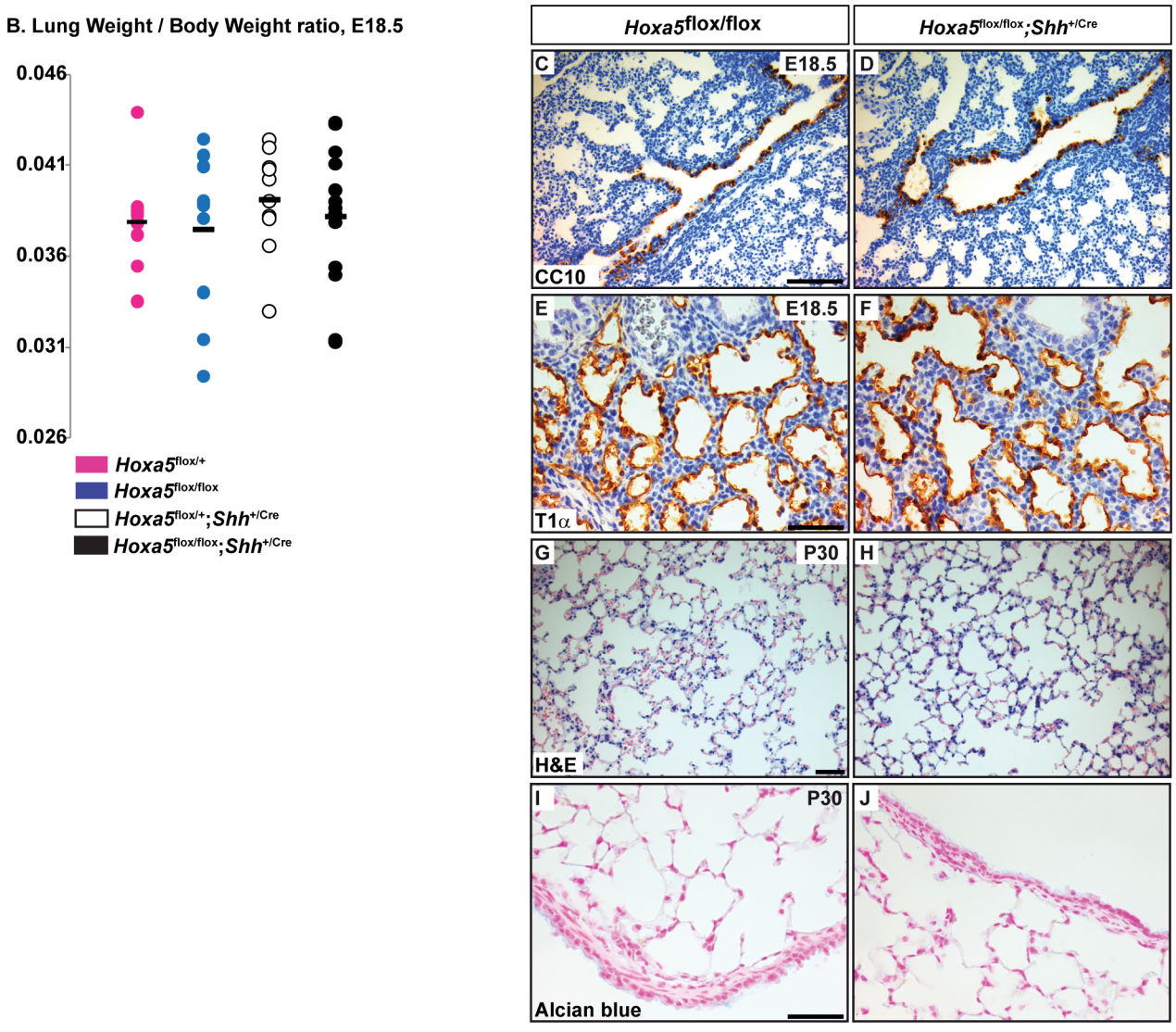

Figure S3

Figure S3. No lung phenotype is caused by the epithelial *Hoxa5* inactivation. Expected mendelian ratios of genotypes of offspring resulting from breeding of *Hoxa5*$^{flox/flox}$ with *Hoxa5*$^{flox/+}$;*Shh*$^{+/cre}$ mice (A). No change was observed for the LW/BW ratio between *Hoxa5*$^{flox/flox}$;*Shh*$^{+/cre}$ embryos and controls at E18.5 (B). No abnormal epithelial cell differentiation of club cells and type I pneumocytes was seen along the respiratory tract of E18.5 *Hoxa5*$^{flox/flox}$;*Shh*$^{+/cre}$ embryos, as assessed by immunostaining for CC10 and T1a, respectively (C-F). Alveolar surface density was normal and no goblet cell metaplasia was detected in lungs from *Hoxa5*$^{flox/flox}$;*Shh*$^{+/cre}$ adults (G-J). These data reflected the lack of *Hoxa5* cell-autonomous function in lung epithelium. Scale bars: 100 µm (C,D,G,H), 50 µm (E,F,I,J).

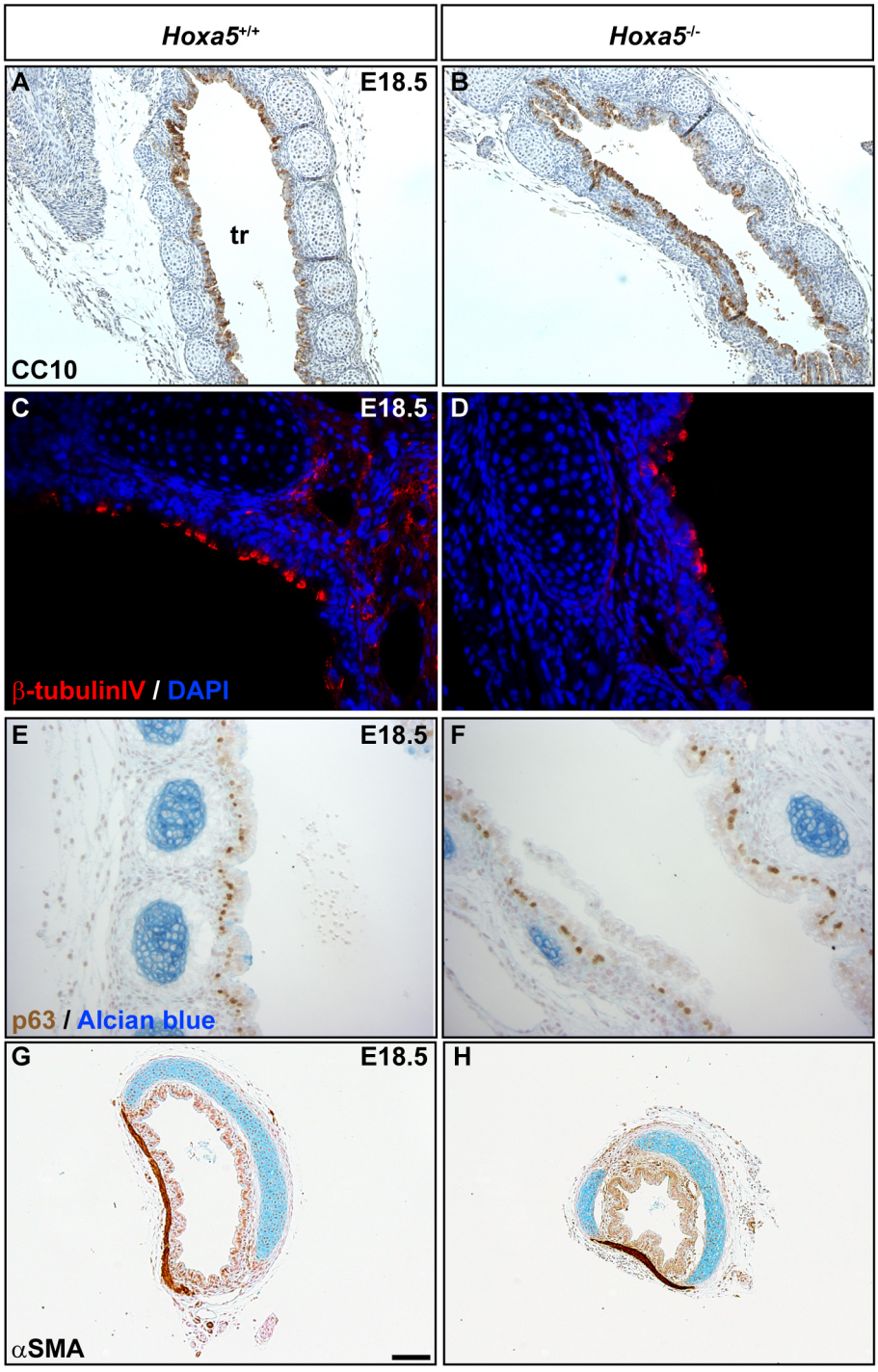

Figure S4

Figure S4. Tracheal smooth muscle formation and epithelial differentiation are unchanged in *Hoxa5*$^{-/-}$ embryos. No quantitative and qualitative variation in club, ciliated, basal, goblet and smooth muscle cells was observed in E18.5 *Hoxa5*$^{-/-}$ tracheas, as assessed by immuno- and histological stainings for CC10, β-tubulinIV, p63, Alcian blue and αSMA, respectively (A-H).

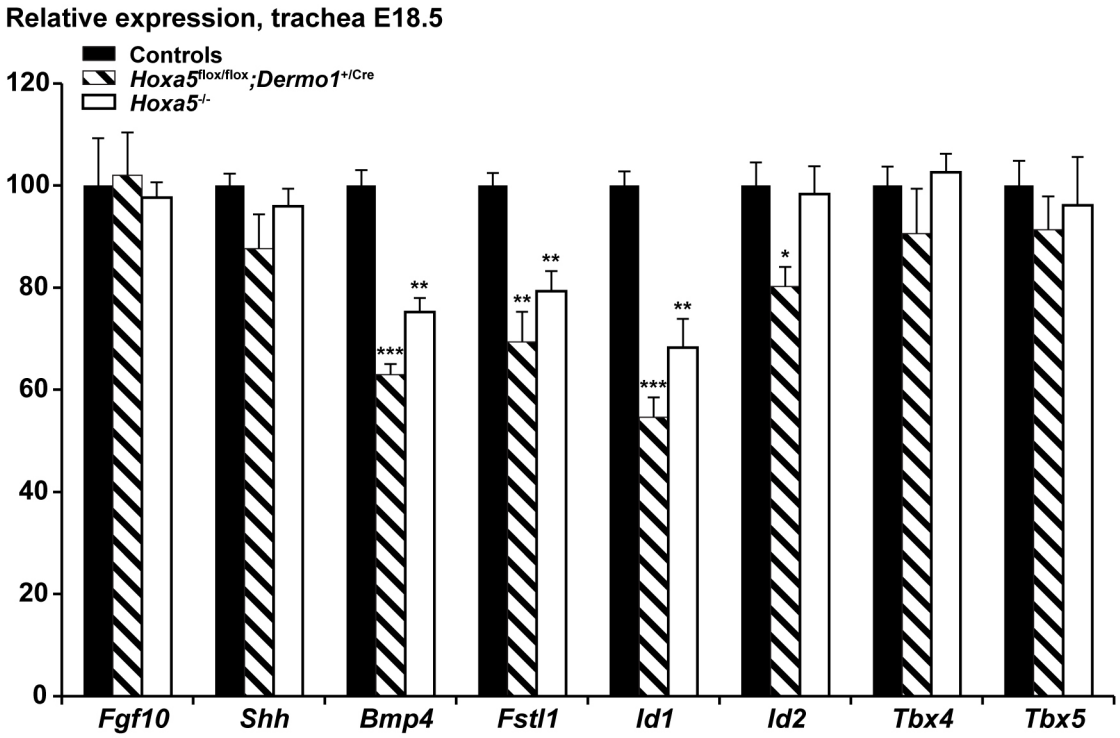

Figure S5

Figure S5. Impact of the loss of *Hoxa5* function on the expression of regulators of tracheal cartilage formation. qRT-PCR analysis of *Fgf10*, *Shh, Bmp4, Fstl1*, *Id1*, *Id2*, *Tbx4* and *Tbx5* expression levels in tracheas from E18.5 wt, *Hoxa5*$^{flox/flox}$;*Dermo1*$^{+/Cre}$ and *Hoxa5*$^{-/-}$ embryos.

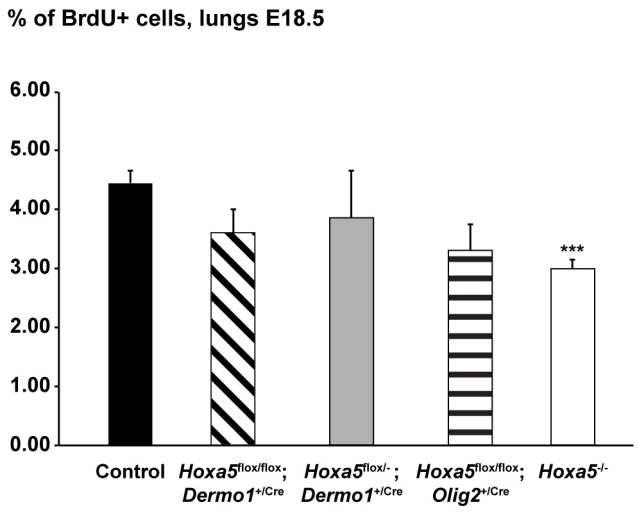

Figure S6

Figure S6. *Hoxa5* mesenchymal and motor neuron mutations differentially influence proliferation of the developing lung. Percentage of BrdU+ cells revealed a downward trend in cell proliferation in E18.5 *Hoxa5*$^{flox/flox}$;*Dermo1*$^{+/Cre}$, *Hoxa5*$^{flox/-}$;*Dermo1*$^{+/Cre}$ and *Hoxa5*$^{flox/flox}$;*Olig2*$^{+/Cre}$ lungs and a significant reduction in *Hoxa5*$^{-/-}$ mutants compared to controls.

A. Relative expression, Lungs E12.5

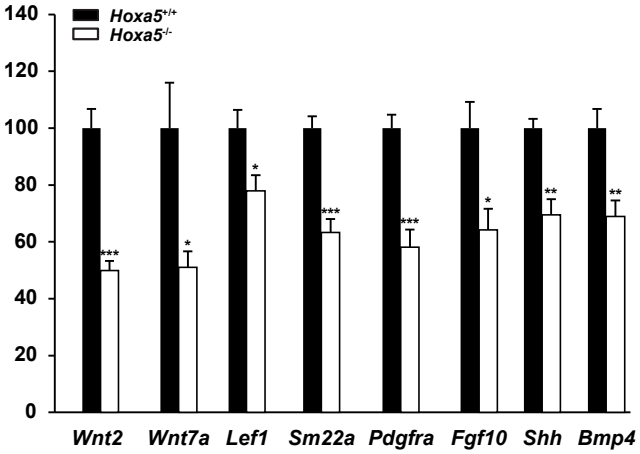

B. Relative expression, Lungs E18.5

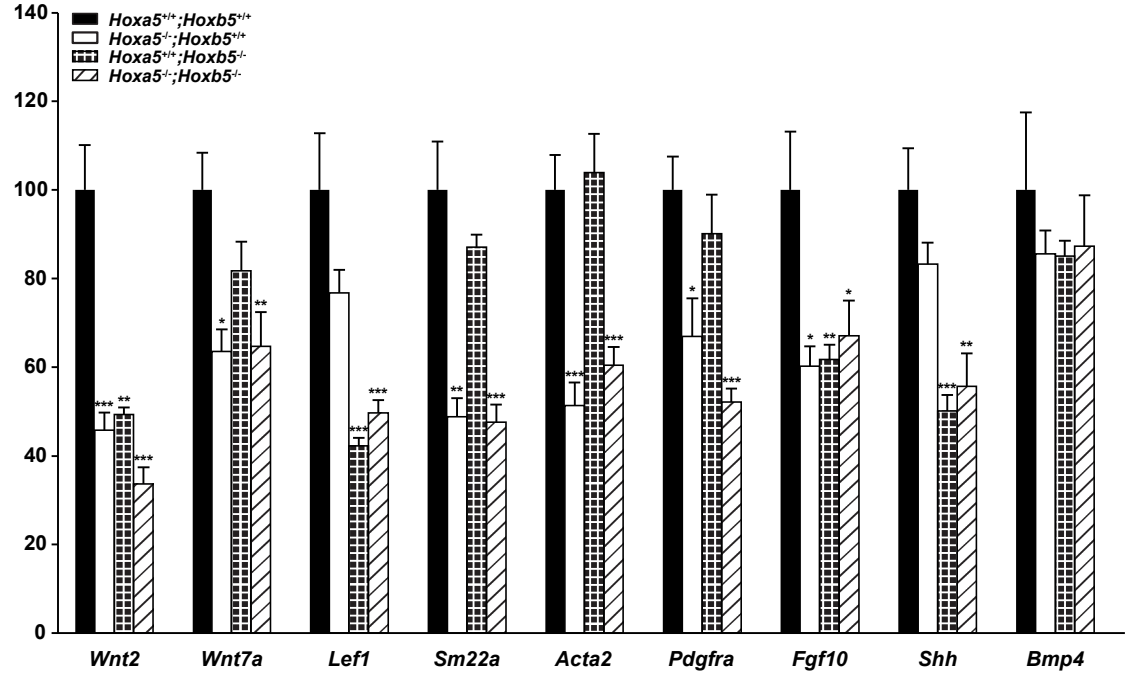

C. Relative expression, Lungs E18.5

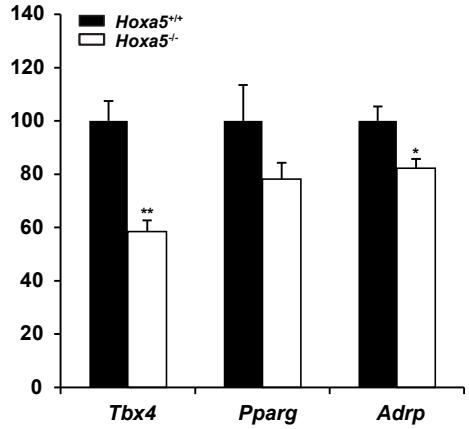

Figure S7. Specific contribution of *Hoxa5* in the control of lung signaling pathways. Expression levels of *Wnt2, Wnt7a, Lef1, Sm22a, Pdgfra, Fgf10, Shh* and *Bmp4* genes in lungs from E12.5 wt and *Hoxa5*$^{-/-}$ embryos (A). All these genes showed a significantly decreased expression in *Hoxa5*$^{-/-}$ lungs. Expression levels of *Wnt2, Wnt7a, Lef1, Sm22a, aSma, Pdgfra, Fgf10, Shh* and *Bmp4* genes in lungs from E18.5 wt, *Hoxa5*$^{-/-}$, *Hoxb5*$^{-/-}$ and *Hoxa5*$^{-/-}$;*Hoxb5*$^{-/-}$ compound mutant embryos (B). *Hoxa5*$^{-/-}$ specimens showed significantly reduced expression levels for *Wnt2, Wnt7a, Sm22a, aSma, Pdgfra* and *Fgf10* while *Hoxb5*$^{-/-}$ specimens showed decreased expression levels for *Wnt2, Lef1, Fgf10* and *Shh.* In *Hoxa5*$^{-/-}$;*Hoxb5*$^{-/-}$ compound mutants, except for *Bmp4*, all genes tested showed a significant reduced expression. Expression levels of *Tbx4*, *Pparg* and *Adrp* genes in lungs from E18.5 wt and *Hoxa5*$^{-/-}$ embryos (C). *Tbx4* and *Adrp* genes showed a significantly decreased expression in *Hoxa5*$^{-/-}$ lungs, while *Pparg* showed a downward trend.

Supplementary Table 1. List of primary and secondary antibodies

Antigen	Antibody/clone	Reference	Source	Dilution
AQP5 (Aquaporin 5)	rabbit polyclonal	Ab78486	Abcam, Toronto, ON, Canada	1:400
αSMA	rabbit polyclonal	Ab5694	Abcam, Toronto, ON, Canada	1:300
BrdU	mouse monoclonal/ clone 131-14871	MAB4072	Millipore, Billerica, MA, USA	1:1000
α-bungarotoxin, Alexa Fluor 555 conjugate		B35451	Invitrogen, Carlsbad, CA, USA	1:1000
βIV-Tubulin	Mouse monoclonal clone ONS1A6	MU178-UC	Biogenex, Fremont, CA, USA	1:150
CC10	goat polyclonal		Gift from Dr. G. Singh, Pittsburg, PA, USA	1:400
Collagen Type II	Mouse/clone II-II6B3. Supernatant		Hybridoma Bank, IO, USA	1:75
HOXA5	rabbit polyclonal	HPA029319	Sigma Aldrich, Oakville, ON, Canada	1:1000
HOXA5	rabbit polyclonal		From Dr. J. Dasen, NY, USA	1:10000
α-Laminin	rabbit polyclonal	BRL#6265SA	Gift from Dr. N. Marceau, Qc, Canada	1:50
Neurofilament (NF)	rabbit polyclonal	AB1987	Millipore, Billerica, MA, USA	1:1000
PAX7	mouse monoclonal		Hybridoma Bank, IO, USA	1:10
p63	mouse monoclonal clone 4A4	Sc-8431	Santa Cruz, Santa Cruz, CA, USA	1 :100
RFP (DsRed)	rabbit polyclonal	600-401-379	Rockland, Limerick, PA, USA	1: 200
SOX9	rabbit polyclonal	sc-20095	Santa Cruz, Santa Cruz, CA, USA	1:100
Synaptophysin (SYN)	rabbit polyclonal	08-0130	Invitrogen, Carlsbad, CA, USA	1:5
T1α	syrian-hamster/ clone 8.1.1. Supernatant		Hybridoma Bank, IO, USA	1:75
Biotinylated goat anti-rabbit		BA-1000	Vector Laboratories, Burlington, ON, Canada	1:250
Biotinylated swine anti-goat		CLCC50015	Cedarlane, Burlington, ON, Canada	1:250
Biotinylated goat anti-syrian hamster		107-065-142	Cedarlane, Burlington, ON, Canada	1:250
Biotinylated goat anti-mouse		115-065-003	Cedarlane, Burlington, ON, Canada	1:500
Donkey anti-rabbit, Alexa Fluor 488 conjugate		A-21206	Invitrogen, Carlsbad, CA, USA	1:1000
Goat anti-mouse, Alexa Fluor 647 conjugate		A-21236	Invitrogen, Carlsbad, CA, USA	1:500
Goat anti-rabbit, Alexa Fluor 488 conjugate		A11008	Molecular Probes, Eugene, OR, USA	1:250
TSA Cyanine 3 Plus Evaluation Kit		NEL744E001KT	PerkinElmer, MA, USA	1:50

Supplementary Table 2. List of primer sequences

Gene	Sequence (5'-3')	Fragment size (bp)
Acta2 (aSma)	F-ACAGCTATGTGGGGGATGAA R-GTTGGCCTTAGGGTTCAGTG	194
Adrp (Plin2)	F-GTCCCTCAGCTCTCCTGTTA R-ATAAGCGGAGGACACAAGGT	146
Bmp4	F-AGCGTCCCGCCAGCCGA R-CGGAGCTCTGCCGAGGAG	148
Col2a1	F-TGGGAATGTCCTCTGCGATG R-TGCCCCTTTGGCCCTAATTT	135
Fgf10	F- TCAAAGCCATCAACAGCAACTATT R-CTCTTTCAGCTTACAGTCGTTGTTAAA	95
Fstl1	F-ATGGCGACTCTCACCTGGAC R-CAATGAGGGCGTCAACACAG	135
Hoxa5	F- CCCAGATCTACCCCTGGATG R- GGCATGAGCTATTTCGATCCT	173
Igf2	F- CCGTACTTCCGGACGACTT R- ATCAGGGGACGATGACGTTT	181
Id1	F-CATGAACGGCTGCTACTCAC R-GAACACATGCCGCCTCG	236
Id2	F-CCTGCATCACCAGAGACCTG R-GGGAATTCAGATGCCTGCAA	102
Lef1	F-AAATGGGTCCCTTTCTCCAC R-CTCGTCGCTGTAGGTGATGA	107
Myf5	F- CCCACCTCCAACTGCTCT R- GCAATCCAAGCTGGACACG	144
Myf6 (Mrf4)	F- ACCCCTACAGCTACAAACCC R- TGCTCCTCCTTCCTTAGCAG	131
Myh1	F- CCGAAGGCGGAACTACTGTAA R- CAGGCTGCATAACGCTCTTT	148
Myh2	F- CAGTGTCTAAGGGCCAAGGGA R- GCCTGGAAAATTCACCGGAT	159
Myh3	F- TTCGCTACAACAGATGCGGA R- CTGGGGTCTTGGTTTCGTTG	175
Myh4	F- TGCTTACGTCAGTCAAGGTGAA R- CATCTGCACTGAATCCCAGG	104
Myh7	F- GGTGGATGATCTGGAGGGAT R- GAGTGCATTTAACTCAAAGTCCTTC	181
Myh8	F- TGAGGAGGCTGAGGAACAATC R- TTACTCTGCGCTGATTTTGGT	160
Myod1 (Myod)	F- GCTCTGATGGCATGATGGATTA R- TGGAGATGCGCTCCACTATG	165
Myog	F- GCCATCCAGTACATTGAGCG R- GTGGGAGTTGCATTCACTGG	123
Pax3	F- GGCGGCAGCAAACCC R- AGGGCACAGTGTTCCGAT	145
Pax7	F- ATTAGCCGAGTGCTCAGAATCA R- CCCTCATCCAGACGGTTCC	140
Pdgfra	F- CCATGCAGTTGCCTTACGACT R- AGAGCCTGCTTTTCACTAGACC	193
Runx1	F- ATGGCAGGCAACGATGAAAA R- AGACGGTGATGGTCAGAGTG	142
Pparg	F-GCCGAGTCTGTGGGGATAAA R-AGGCACTTCTGAAACCGACA	181
Shh	F-TGACTCAGAGGTGCAAAGACA R-ACTCCTCTGAATGATGGCCG	120
Sox5	F-CACCCTGAAGCAGAGGAAGA R-GGCTCTCAGGAGTCCCTTTT	152
Sox6	F-AATTCTTCAGGCCTTCCCTGAC R-CTTAGCCGGGCCTGTTCTTC	219
Sox9	F-GTCGGTGAAGAACGGACAAG R-CTGAGATTGCCCAGAGTGCT	157
Tagln (Sm22a)	F-TGGCTGAAGAATGGTGTGATTC R-TTGAGCCACCTGTTCCATCT	126
Tbx4	F-TCCTACCAGAACCACAAGATCAC R-CCCATTCTCATACTGGTAGTGC	240
Tbx5	F-CCGGAGACAGCTTTTATCGC R-ACTCTTTACTTTGCATCCGAGAC	145
Wnt2	F-TGATGTAGACGCAAGGGGG R-GCCACCTGTAGCTCTCATGTA	129
Wnt7a	F-CACAATAACGAGGCGGGTC R-TCCAGCACGTCTTAGTGGTA	100